FULL PAPER

Polywraplex, Functionalized Polyplexes by Post-Polyplexing Assembly of a Rationally Designed Triblock Copolymer Membrane

*Xuemei Ge, Shiyue Duan, Fei Wu, Jia Feng, Hua Zhu, and Tuo Jin**

A core–shell structured synthetic carrier, polywraplex, is reported to overcome the hurdles along the inter- and intracellular pathways of systemic delivery of siRNA, yet remain structurally simple and easy-to-formulate. The core is a cationic polyplex formed of siRNA with polyethylene imine (PEI) and polyspermine-imidazole-4,5-imine (PSI), respectively, and the shell is a self-assembled unilamella membrane of PEG_{45}-PCL_{20}-mototriose-COO^-, a triblock copolymer possessing multicarboxyl saccharide block to guide adsorption to each polyplex surface, a hydrophobic central block to form a protecting layer around the nucleic acid core, and a PEG block functioning as a steric stabilization out-layer to extend in vivo circulation. The hydrophobic layer limits the anionic charges of the guiding block within a 2D surface to prevent them from penetrating into the polyplex, a common cause for prephagocytic siRNA leaking by polyelectrolytes in vivo. Cell targeting agents may be conjugated to the distal end of the PEG block and assembled on polyplex surface in optimal population. Chemical characterizations comprising consequent fluorescent imaging, dynamic laser scattering, zeta potential, as well as electrophoresis confirm polywraplex formation and its protection to siRNA against leaking and degradation in serum. Cellular and in vivo (mice) assays of biotin-conjugated polywraplexes suggest prolonged circulation and tumor tissue targeting.

1. Introduction

The critical roadblock in converting siRNA from therapeutic actives to medicines is our inability to date to deliver them to therapeutic sites safely and efficiently.[1,2] A therapeutically feasible synthetic delivery system must accomplish all the essential tasks along the in vivo pathway as A) packing them into nanoparticulates to avoid prephagocytic degradation; B) adsorbing onto target cells selectively; C) escaping from endosomal digestion after uptake; D) releasing the nucleic acids at intracellular acting sites; and (E) metabolizing itself to nontoxic species.[3,4] Incorporating all the capabilities to meet these tasks within a synthetic carrier of fairly simple structure through an easy-formulating process is essential but highly challenging.

Rationally designed RNA with a loop of complementary sequences may complement to each other specifically to form a self-protective nanoparticle stable in circulation and phagocytosable by target cells.[5,6] These RNA could self-assembly nanoparticulates may serve as a useful vehicle to delivery siRNA of known number of copies to the target cells by conjugating with defined number of siRNA and cell-targeting aptamers on their "Y" or "X" shaped arms. For post-phagocytic process, however, the assistance by endosome rupturing agents may be desired. An improvement was made to such RNA assemblies by enhanced stability and fluorogenic linking sites recently.[7] These newly developed nature may be utilized to conjugate more functional components to the particles.

Conjugating the required functional components to cationic polymers or lipids prior to assembling with nucleic acids into the nanoparticles such as polyplexes, lipopolexes, or micelleplexes is a well-reported strategy.[8–14] It is, however, difficult for a cationic packing agent conjugated with multiple components to condense siRNA into particles of desired size, efficiency, and prephagocytic stability.[13–15] Various post-polyplexing or post-lipoplexing modifications were therefore proposed.[16,17]

Wrapping a cationic polyplex with a negatively charged lipid bilayer as strategy to form the protective and functional surface (e.g., lipopolyplex-II) was reported.[18] Instability of this electrostatic attachment may limit its in vivo applications. Preconjugating cyclodextrin to the backbone of a cationic polymer resulted in polyplexes possessing molecular "plugs" on the surface to allow adamantine-conjugated cell-targeting agents or steric stabilization agents to be attached through post-polyplexing insertion.[19–21] The drum-shaped cyclodextrin (1.53 nm in diameter) conjugated on the backbone of the polymer may, however, reduce the efficiency of siRNA condensation and lead to polyplexes loose in structure. Adsorbing a layer of negatively charged polyelectrolyte at the surface may help to condense the oppositely charged loose polyplexes. But replacement of the loaded siRNA due to its similar poly-anionic nature may become a problem.[22,23] Nanoencapsulation with various functional agents is alternative strategy in addition to

Dr. X. Ge, Dr. S. Duan, Dr. F. Wu, J. Feng, Prof. T. Jin
Center for BioDelivery Sciences, School of Pharmacy
Shanghai Jiao Tong University
800 Dongchuan Rd, Shanghai 200240, P. R. China
E-mail: tjin@sjtu.edu.cn
Prof. H. Zhu
Department of Microbiology and Molecular Genetics
New Jersey Medical School
Rutgers University
225 Warren Street, Newark, NJ 070101, USA

DOI: 10.1002/adfm.201500724

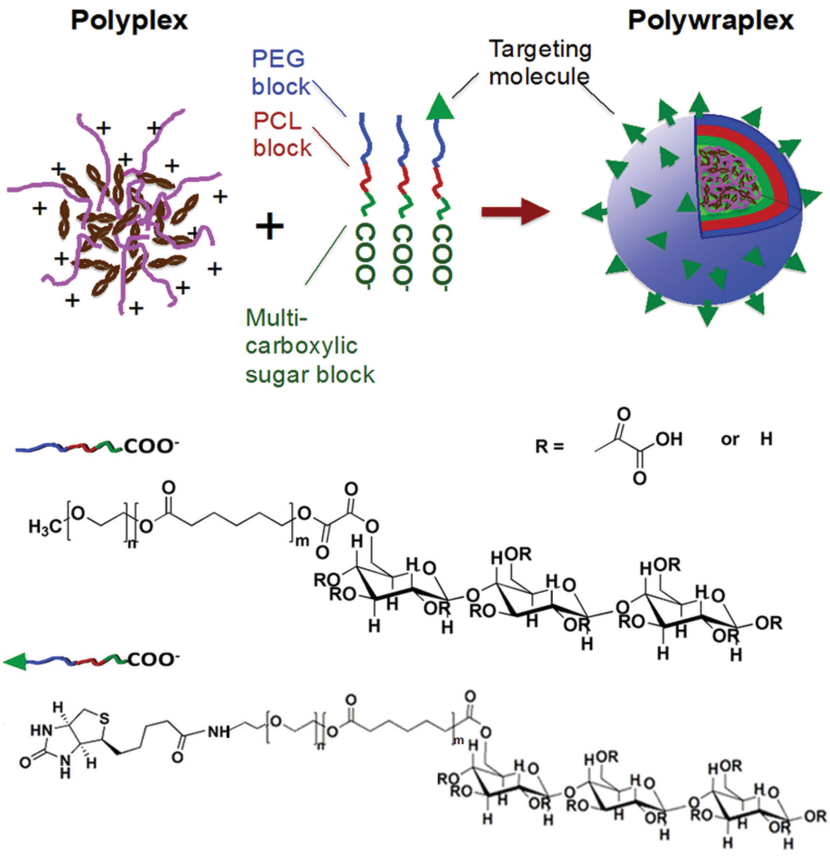

Figure 1. Schematic description of polywraplex formation using rationally designed triblock copolymer (mPEG45-PCL20-maltotriose-COO$^-$ and biotin-PEG45-PCL20-maltotriose-COO$^-$) to form the functional surface. Approximately 70% of the trisaccharide hydrogels were carboxylated with oxalyl chloride (followed by hydrolysis) as confirmed by its NMR spectra (Figures 2 and 3).

self-assembly, but organic solvents are needed to overcome the missing mechanism for nucleic acid condensation.[24,25]

To form protective and stable functional surface, post-polyplexing reactions comprising post-adsorbing polymerization, click reactions with the surface of already-formed polyplex or lipopolyplex, and di-sulfide bridging of polyplex-forming materials were proposed. While these methods may efficiently stabilize the nanoparticles in terms of preventing nucleic acid leaking and particle enlargement due to zeta potential change, the reaction-involved formulation process and the need to pre-conjugate reactive groups to the siRNA packing materials may raise some regulatory concerns and limit selection of cationic polymers.[17,26,27]

We reported recently a chemically dynamic and biologically responsive poly-cationic carrier, which may pack siRNA and accomplish all the intracellular tasks (C, D, E) successfully.[28] To accomplish the intercellular delivery, we hereby demonstrate a nonreactive, solvent-free, and easy-to-formulate method to assemble a highly functional membrane around an already-formed polyplex of any content for intercellular targeting on the basis of the reported advances in post-polyplexing functionalization (**Figure 1**). This membrane was formed from a rationally designed triblock copolymer consisting a multicarboxyl surge block to guide the surface assembly, a hydrophobic central block to form an isolating layer around the polyplex,[29] and a PEG chain to function as the steric stabilization agent.[30,31] The hydrophobic layer is essential also for restraining the negative charges of the guiding block within a 2D surface to prevent their interpenetrating into the polyplex core, a cause for replacement of the loaded siRNA. Cell-targeting moieties may be immobilized on the carrier by conjugating to the distal end of the PEG block prior to the self-assembly. We name this membrane-wrapping polyplex as "polywraplex."

2. Results

2.1. Synthesis of mPEG-PCL-Maltotriose-COO$^-$ and Biotin-PEG-PCL-Maltotriose-COO$^-$

As described in **Figure 2**a, synthesis of mPEG$_{45}$-PCL$_{20}$-maltotriose-COO$^-$ started with opening polymerization of ε-carprolactone using mPEG$_{45}$-OH or mPEG$_{45}$-COOH as the nucleophilic initiator, followed by conjugating maltotriose to the end of the polycarprolactone (PCL) block. For mPEG$_{45}$-OH induced polymerization, the formed diblock copolymer, mPEG$_{45}$-PCL$_{20}$-OH, was preactivated with oxalyl chloride prior to the reacting with maltotriose. In the case of mPEG$_{45}$-COOH, the formed mPEG$_{45}$-PCL$_{20}$-COOH was allowed to condense with maltotriose directly in the presence of BOP. The remaining maltotriose hydroxyls of the formed triblock copolymer, mPEG$_{45}$-PCL$_{20}$-maltotriose, were finally carboxylated with excess oxalyl chloride, followed by hydrolysis of the dangling acyl chloride. Formation of the intermediate of each reaction step and the final product, mPEG$_{45}$-PCL$_{20}$-maltotriose-COOH, were confirmed using ^{1}H NMR spectroscopy (Figure 2b). The chemical shift at 3.51 ppm was attributed to methylene unit in PEG segment and the signal at 3.98 ppm was assigned to α-methylene unit in the PCL block. The group of peaks for the hydroxyls of maltotriose (4.2–6.0 ppm) indicated formation of mPEG$_{45}$-PCL$_{20}$-maltotriose. Carboxylation of the maltotriose block was confirmed by the dramatic decrease in the hydroxyl peaks in the ^{1}H NMR spectra (4.2–6.0 ppm, Figure 2b).

To conjugate biotin (vitamin H recognized as a growth promoter responsible for rapid proliferation of tumor) to the triblock copolymer, biotin-CO-NH-PEG-COOH was used instead of mPEG-OH or mPEG-COOH as the initiator for ε-carprolactone ring opening (**Figure 3**a). Biotin-CO-NH-PEG-COOH was synthesized by activating the biotin carboxyl with hydroxysuccinimide (NHS), followed by coupling with NH$_2$-PEG-COOH to form the amide linkage (Figure 3a). Formation of the key intermediates and the final product, biotin-CO-NH-PEG-PCL-maltotriose-COOH, was determined by the ^{1}H NMR spectra shown in Figure 3, as well as the fragments of their mass spectrum at m/z 364 [M+Na]$^+$ and m/z 342 [M+H]$^+$(Figure S1, Supporting Information).

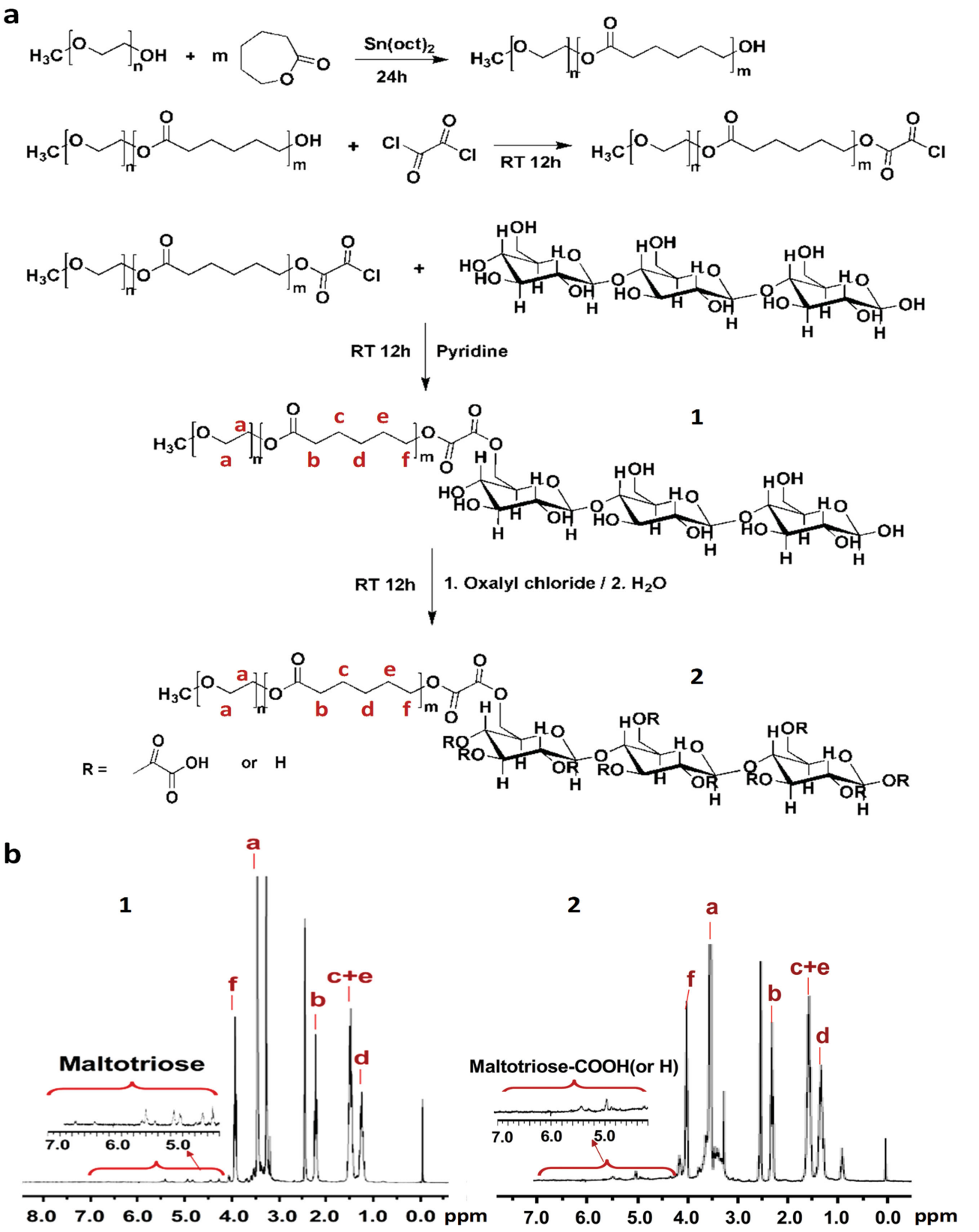

Figure 2. a) Synthetic procedure of copolymer, mPEG45-PCL20-maltotriose-COO^-. b) ^1H NMR spectra of the triblock copolymers 1. mPEG45-PCL20-maltotriose and 2. mPEG45-PCL20-maltotriose-COO^- in synthesis (NMR solvent: DMSO-*d*6).

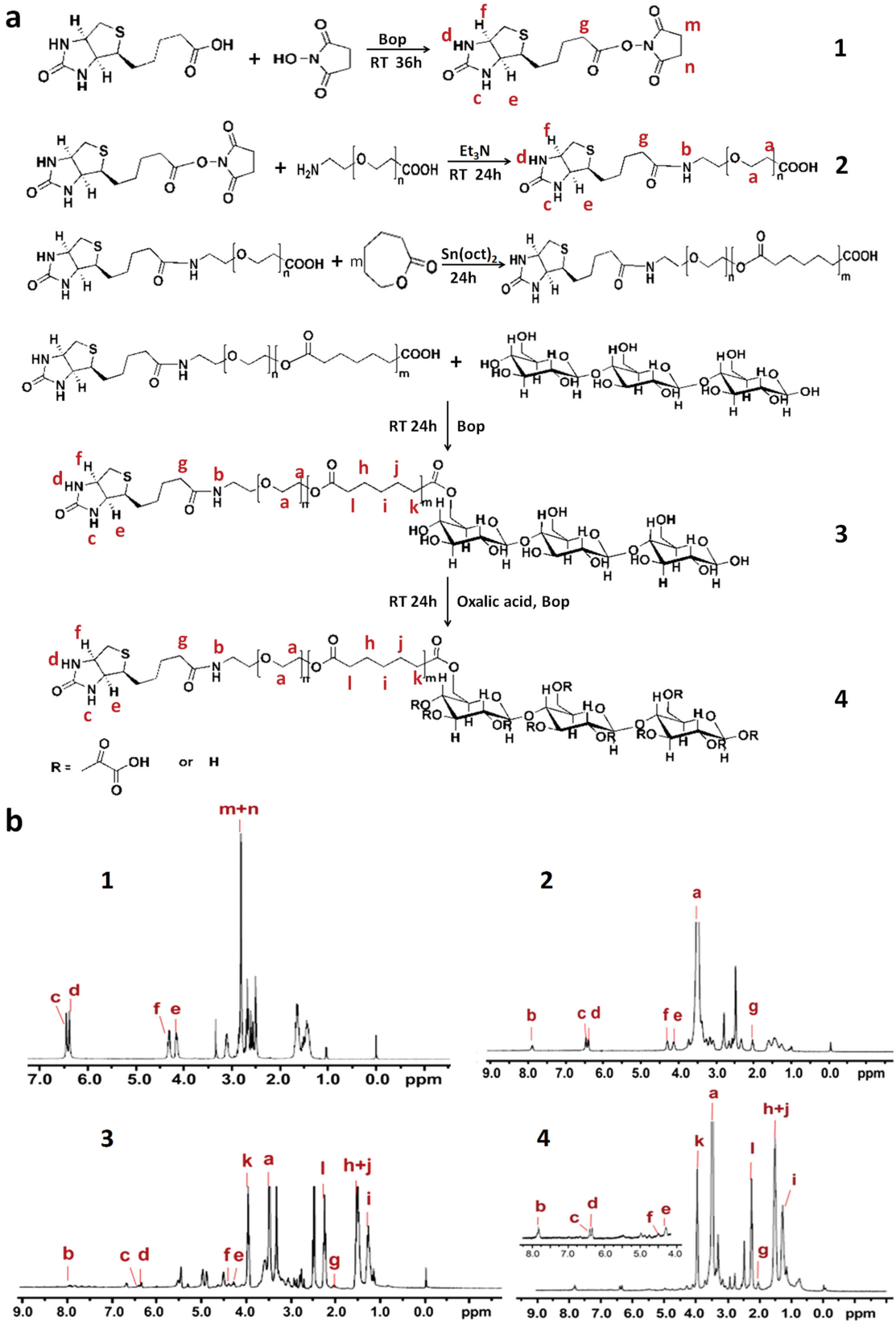

Figure 3. a) Synthetic procedure of copolymer, biotin-PEG45-PCL20-maltotriose-COO⁻. b)[1]H NMR spectra of the triblock copolymers 1. Biotin-NHS, 2. Biotin-PEG45, 3. Biotin-PEG45-PCL20-maltotriose, and 4. Biotin-PEG45-PCL20-maltotriose-COO⁻in synthesis (NMR solvent: DMSO-*d*6).

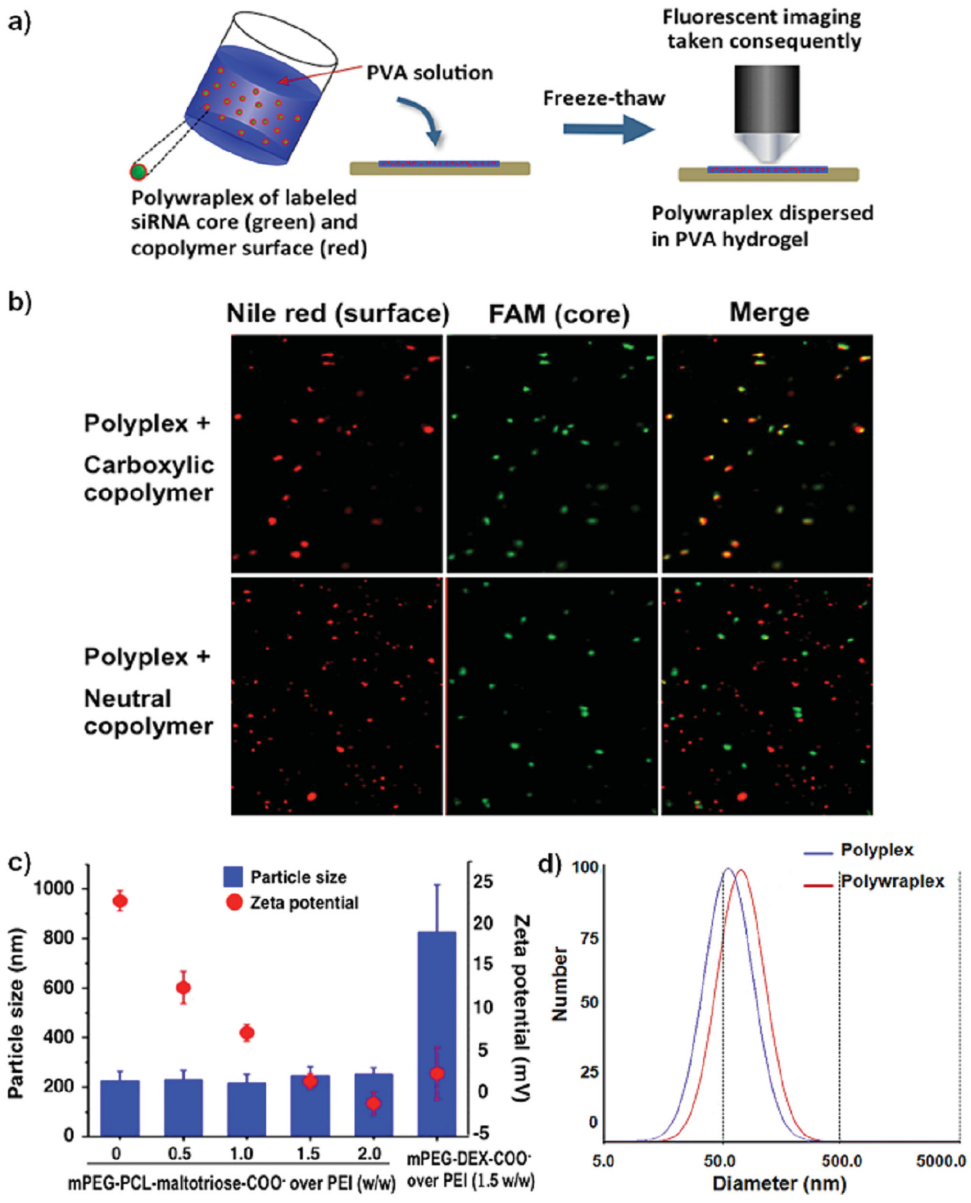

Figure 4. a) Experiment setup for fluorescent imaging of polywraplexes. b) Fluorescent images of polywraplexes immobilized in PVA hydrogel. The polyplexes formed of PEI-25KD and FAM-conjugated siRNA (green) were treated with mPEG45-PCL20-maltotriose-COO⁻ and mPEG45-PCL20-maltotriose, respectively. Nile red was added during the copolymer treatment for partitioning into the hydrophobic phases formed. c) Particle sizes and zeta potential of polywraplex formed of PEI-siRNA core (1:1 of w/w ratio) wrapped with different mass ratio of block copolymer, mPEG45-PCL20-maltotriose-COO⁻, and that of the polyplex wrapped with a diblock copolymer, PEG-DEX-COO⁻. d) Particle size distribution of polyplex and polywraplexes (mPEG-PCL-maltotriose-COO⁻:PEI = 1.5:1).

2.2. Formation of Polywraplexes Through Nonreactive Self-Assembly

Formation of polywraplex was confirmed by comparing the fluorescent images for the core and the surface of the nanoparticles which were labeled, respectively, with carboxyfluorescein (FAM, green, conjugated on anti-pGL3 siRNA) and Nile red (red, partitioned in the PCL layer). For proof-of-concept, polyethylene imine (PEI-25KD), a well-reported polycationic gene packaging agent, was used to form the polyplex core with the labeled siRNA. Then $mPEG_{45}$-PCL_{20}-maltotriose-COO^-, the triblock copolymer, and Nile red, a hydrophobic dye, which may partition in the hydrophobic matrix of PCL, were added to the polyplexes. Since the nanometer-sized core–shell structure cannot be resolved under an optical microscope, its formation was visualized by fluorescent images of immobilized particles taken consequently using different incident lasers. The particle immobilization was achieved by suspending polywraplexes in a polyvinyl alcohol (PVA) solution, followed by gelation through a freeze–thaw treatment (**Figure 4**a). The immobilized polywraplexes were therefore imaged under a fluorescent microscope using incident lasers of 460–495 nm and 530–550 nm for the green core and the red surface, respectively. As shown

in Figure 4b, the two fluorescent images taken consequently for the self-assembled polywraplexes are overlapped perfectly, indicating the attachment of the copolymer around the nanoparticles. On the contrary, when the polyplexes were treated with PEG_{45}-PCL_{20}-maltotriose, the same copolymer without the carboxyl groups on the sugar guiding block, the green dots, and the red dots dispersed independently (Figure 4b), suggesting that the carboxyl-free triblock copolymer aggregated to micelles. This result consists with our hypothesized physical chemistry of polywraplex formation in Figure 1: presence of cationic nanoparticle surfaces will guide the anionic triblock copolymer, $mPEG_{45}$-PCL_{20}-maltotriose-COO^-, to form a stable membrane around each particle rather than self-aggregate to micelles or complex with PEI by replacing siRNA. In another word, self-consisting between the two 2D processes, alignment of the PCL block to a unilamella layer and the ionic interaction between polyplex surface and aligned carboxyl array, gained thermodynamic preference.

The formation of polywraplex was further confirmed by particle size and zeta potential measurement using dynamic laser scattering (DLS). As shown in Figure 4c, adding $mPEG_{45}$-PCL_{20}-maltotriose-COO^- to the polyplexes resulted in zeta potential drop of from 22.8 to 1.8 mV, but not an increase in the average diameter of the nanoparticles accordingly. This result indicates that the polyanionic triblock copolymer adsorbed on the surface of each cationic polyplexes and compressed the loose polyplex core by the interaction between the opposite charges. On the contrary, when PEG_{45}-$DEX_{3.5k}$-COO^-, a di-block copolymer consisting a PEG chains and a multi-carboxyl dextran block but without the hydrophobic PCL in between, was added to the same polyplexes, the average particle sizes increased dramatically as expected from 200 to 800 nm as the zeta potential approached zero from 25 mV (Figure 4c,d). It is well observed that polyplexes are highly dynamic in size depending on polyplex-forming polymers, zeta potential, and interaction with ionic modifiers.[32,33] This instability was, however, prevented by the ionic adsorption of the rationally designed triblock copolymer in which the hydrophobic central block of $mPEG_{45}$-PCL_{20}-maltotriose-COO^- played a critical role in forming a stable unilamella membrane around each polyplex.

To examine the applicability of the triblock copolymer membrane in encapsulating polyplexes formed from different cationic polymers with varying amino group density and weight ratio to siRNA, the self-assembly process was carried out over polyplexes formed of polyspermine-imidazole-4,5-imine (PSI), and subjected to the same characterizations. PSI is structured as 145 molecular weight units per amino group (3.3 times as that of PEI), and the weight ratio over siRNA was set as 25:1 for assembling the $mPEG_{45}$-PCL_{20}-maltotriose-COO^-membrane. As indicated in **Figure 5**, the fluorescent dots for, respectively, labeled green core and red shell were overlapped as completely as those of PEI polywraplexes (Figure 4a), and the zeta potential of the PSI polyplexes dropped to nearly zero without increase in the particle sizes when being treated with the triblock copolymer. The similar results upon the block copolymer assembly over the PEI and PSI polyplexes (Figures 4 and 5) strongly suggest that this nonreactive polyplex functionalization strategy is broadly applicable.

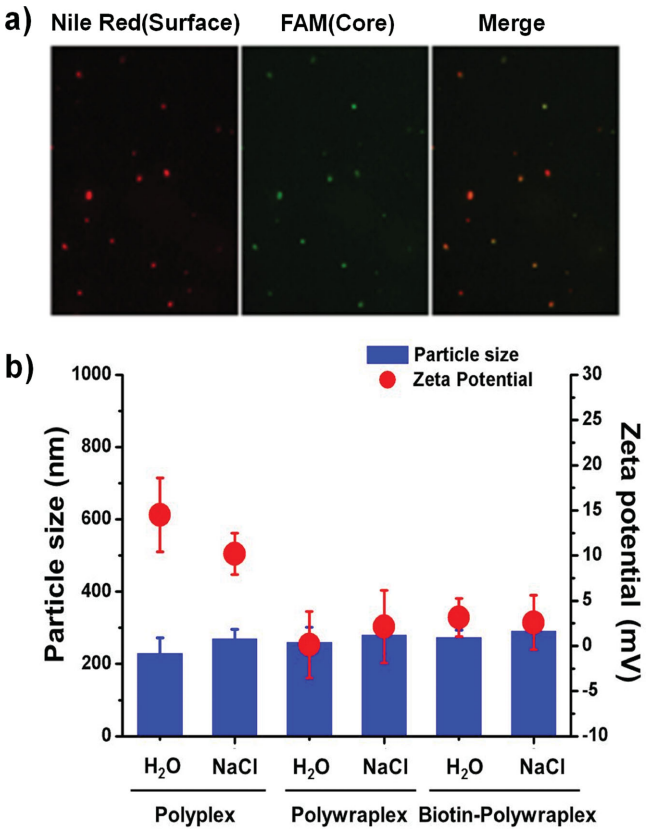

Figure 5. a) Fluorescent microscopic images of polywraplexes immobilized in PVA hydrogel. The polyplex core formed of PSI and FAM-conjugated siRNA (green) was treated with PEG45-PCL20-maltotriose-COO^-in the presence of Nile red for imaging the hydrophobic domain formed of the PCL block. b) Particle sizes and zeta potential of the polywraplexes formed of PSI-siRNA core (25:1 of w/w ratio) wrapped with block copolymer mPEG45-PCL20-maltotriose-$COO^-$and biotin-PEG45-PCL20-maltotriose-COO^-.

2.3. Protective Effect of $mPEG_{45}$-PCL_{20}-Maltotriose-COO^- Membrane to siRNA Core

The capability and efficiency of the self-assembled triblock copolymer membrane in protecting the encapsulated nucleic acids against in anionic polyelectrolytes and digesting enzymes were examined by incubating siRNA-loaded polywraplexes with calf thymus DNA and calf serum, respectively. As indicated by the electrophorograms in **Figure 6**a, the band for leaked siRNA was observed immediately as the bare polyplex was treated with calf thymus DNA as a model of in vivo anionic polyelectrolyte, but no siRNA band was detected for the polymer-wrapped polywraplex. Similarly, when the two particulate samples were both incubated in 50% calf serum (with naked siRNA as the control), the siRNA content in the polyplexes decayed as a function of incubation time in a comparable pace as that of the naked siRNA, but no decay of siRNA content was observed for polywraplex during the 48 h incubation (Figure 6b). Comparison was also made between the siRNA-loaded polyplexes wrapped with the triblock $mPEG_{45}$-PCL_{20}-maltotriose-COO^- and the two-block PEG_{45}-$DEX_{3.5k}$-COO^-, both were incubated in low concentration calf

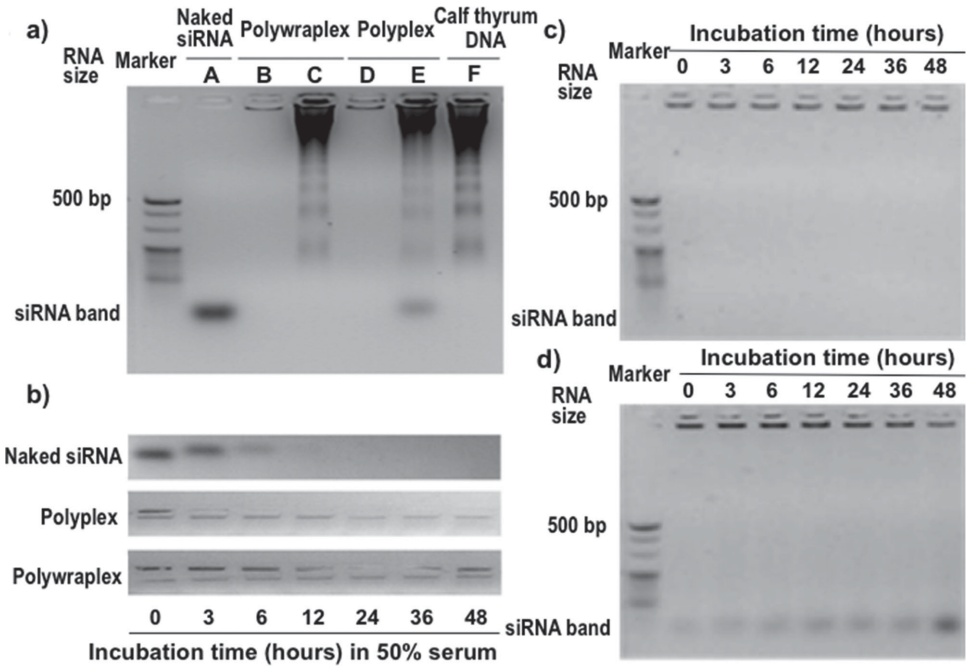

Figure 6. Capability of polywraplex in preventing siRNA leaking and degradation. a) Electrophoresis bands of marker; A: naked siRNA; B: polywraplexes loaded with PEI and siRNA at mass ratio of 1:1; C: polywraplexes as B but treated with calf thymus DNA; D: polyplexes loaded with PEI and siRNA at mass ratio of 1:1; E: polyplexes as D, but treated with calf thymus DNA; F: calf thymus DNA. b) Electrophoresis bands of siRNA in naked form, recovered from polyplexes, and recovered from polywraplexes after being incubated in 50% serum for different time periods. c) PEG-PCL-maltotriose-COO^- membrane polywraplexes loaded with PEI and siRNA at mass ratio of 1:1 treated with calf thymus DNA for different time periods. d) PEG-DEX-COO^- membrane nanoparticles loaded with PEI and siRNA at mass ratio of 1:1 treated with calf thymus DNA for different time periods.

thymus DNA for 48 h. As indicated by the electrophorograms in Figure 6c,d, siRNA leaked from the polyplexes wrapped with the diblock copolymer but not from those wrapped with the triblock copolymer membrane over the experiment time. Clearly, formation of the hydrophobic isolating layer from the PCL block was essential and critical for the stabilizing and protective effect of the surface membrane to the siRNA core. Although electrophoresis is only semiquantitative, the significant difference in siRNA leaking between the polyplexes wrapped with $mPEG_{45}$-PCL_{20}-maltotriose-COO^- and PEG_{45}-$DEX_{3.5k}$-COO^- is meaningful and convincing.

2.4. In Vitro Assays for Cytotoxicity and Silencing Efficiency of Polywraplex

The advantages of polywraplex comprise its compatibility in terms of cytotoxicity and flexibility in selecting cell-targeting agents. Adding the membrane-forming triblock copolymer to a series of cell types resulted in cell viability declining till 2 mg mL^{-1}, a concentration 10–100 times higher than the working concentration of most of nucleic acid transfection agents (**Figure 7**a). Viable cells were determined by measuring the absorbance of the samples at 570 nm (with 630 nm as the reference) using a SpectraMax M3 Multi-Mode Microplate Reader. Cell viabilities were determined with the untreated cells (normal cells) being 100%. Cytotoxicity of already-formed polywraplex particles was also examined by cell viability test prior to gene silencing test. To rule out the toxicity effect of PEI on gene silencing, nontoxic PSI was used to form the polyplex core.[28] As expected from the nontoxicity of the polymeric material as well as the neutral surface charge of stable polywraplex, treatment by the particles did not resulted in cell viability declining (Figure S3b, Supporting Information).

Selected cell-targeting molecule can be conjugated to the distal end of the PEG chain of the triblock copolymer and immobilized on the polyplex surface simply by mixing with targeting molecule-free $mPEG_{45}$-PCL_{20}-maltotriose-COO^- prior to assembling on the polyplex surface. To examine this formulation convenience, biotin, a ligand well used for pretargeting tumor cells, was conjugated to the PEG chain of the triblock copolymer.[34] The biotin-conjugated copolymer, biotin-PEG_{45}-PCL_{20}-maltotriose-COO^- was blended into the biotin-free $mPEG_{45}$-PCL_{20}-maltotriose-COO^- solution in the fractions of 0%,10%, 20%, 30%, 40%, and 50%, and assembled around the polyplex carrying luciferase-silencing anti-pGL3-siRNA. Accordingly, polywraplexes of nearly zero zeta potential and 200–250 nm diameter were formed in saline (Figure S3a, Supporting Information). The formed polywraplexes of various biotin populations were then added to the culture of SMMC-7721 cells stably expressing luciferase pGL3-gene to examine the silencing activity. The expression of luciferase in the test cells was measured using a single-tube luminometer, and luciferase activity of a sample was normalized on protein concentration. The decrease of the enzymatic activity resulted from the polywraplex treatment was plotted against the biotin population on the particle surface in

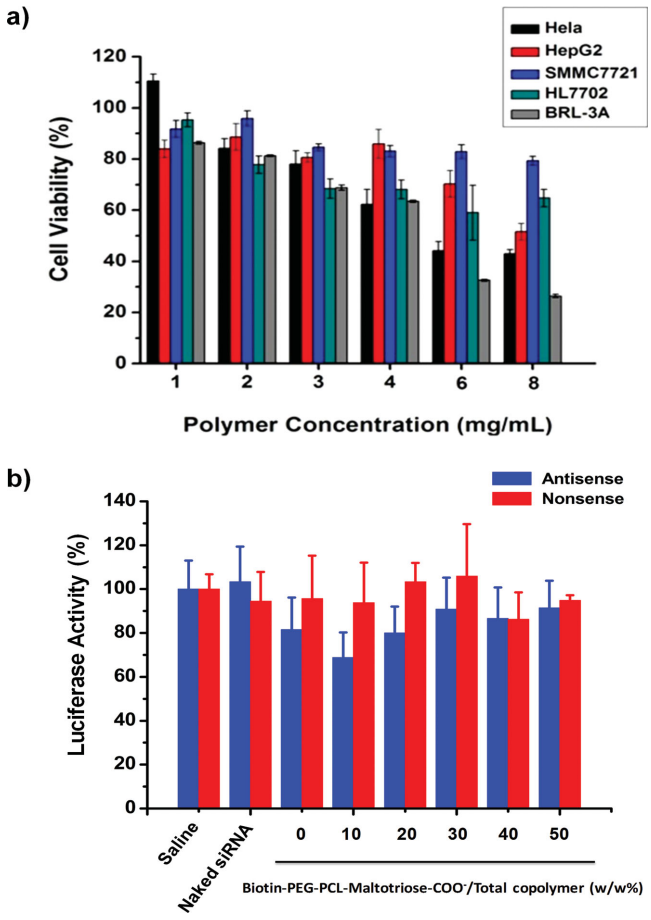

Figure 7. In vitro assays for cytotoxicity and silencing efficiency of polywraplex. a) Viability of HeLa, HepG2, SMMC7721, HL7702, BRL-3A treated with mPEG-PCL-Maltotriose-COOH; b) Efficiency in silencing luciferase gene stably expressed in SMMC-7721 cells by anti-pGL3 siRNA delivered with polywraplexes containing 0%, 10%, 20%, 30%, 40%, 50% of biotin-conjugated copolymer in the surface membrane. The graphical data represent mean±SD (n = 6).

Figure 7b. The polywraplex formed from the triblock copolymers of which 10% were conjugated with biotin showed the maximum luciferase-silencing activity. Selective cell targeting is normally meaningful in vivo where the nanoparticulate carriers are exposed to various cell types.[35,36] The dependence of silencing activity on the population of the targeting agent in the single cell type (Figure 7b) seems not rational. A speculation may be that the biotin may need sufficient population and flexible orientation to bind to target cells, and moderate surface population may meet both of the criteria. Nevertheless, 10% of the biotin-conjugated copolymer was mixed into the total block copolymer in polywraplex formation for successive in vivo studies.

2.5. In Vivo Assays for Silencing Efficiency and Tissue Distribution of Polywraplex

The capability of biotin-conjugated polywraplex to bind tumor cells selectively was examined by injecting this carrier system to BALB/c nude mice implanted with SMMC-7721 cancer cells stably expressing luciferase. The tumor tissues developed from implanted cells were reported to serve as a useful model for examining targeted nucleic acids delivery through EPR (enhanced permeability and retention) effect and cell recognition.[37,38] Again, our recently invented bioresponsible and nontoxic PSI was used to pack the anti-luciferase siRNA into the polyplex core. Prior to injection to the animals, stability of the polywraplexes in serum was confirmed by incubating the nanoparticles in serum solutions at 37 °C for 24 h. As shown in **Figure 8**b, the particle size of the PSI-core polywraplexes remained unchanged over the incubation process, suggesting acceptable in-serum stability. The dosage regimes to each group of the animals include IV injections of saline (control), naked siRNA, biotin-free polywraplex, and biotin– polywraplex, as well as site injection of bare polyplex. As expected, the mice received naked siRNA showed no silencing activity. For the two test groups received biotin–polywraplexes and biotin-free polywraplexes, on the contrary, the luciferase-silencing activity was comparable to that of site-injected bare polyplex, with the former slightly higher than the later. It seems that polywraplexes were retained in the tumor tissue considerably through the EPR effect for which the tumor cells were exposed to sufficient dose from both the two polywraplex dosage forms. It is well agreed that EPR effect targeting tumor tissues requires the diameter of the delivery carriers to be near or less than 100 nm to ensure satisfied efficiency. The EPR effect observed for the polywraplexes over 200 nm in diameter may have served as qualitative comparison between the noncharged polywraplexes and cationic polyplex.[39–41] Nevertheless, since the rationally designed block copolymer may form a multifunctional unilamella membrane around a cationic polyplex of any content and size without enlarging the particle-diameter, formulating a cationic polyplex possessing defined sizes should best fit the polywraplex strategy.

Injecting the five dosage forms (saline, naked fluorescent Cy3-siRNA, bare polyplex, biotin-free polywraplex, and biotin–polywraplex) to experimental mice implanted with SMMC-7721 tumor cells through the tail vein resulted in significantly different tissue distributions (Figure 8c). The animals were sacrificed 12 and 24 h after administration of respective dosage forms, and the organs were dissected and imaged under a fluorescent microscope. As shown in Figure 8c, the Cy3-siRNA administrated in the particulate forms was accumulated more in liver, lung, and the tumor developed from SMMC-7721 cells. Further analysis indicated that biotin–polywraplexes accumulated in the tumor the most, followed by biotin-free polywraplexes and bare polyplexes (Figure 8c). Accordingly more bare polyplexes were accumulated in the liver. Extending the circulation time from 12 to 24 h led to dramatic decrease of the Cy3-siRNA accumulation in the liver for all the animals, but a significant increase in the tumor tissue for the mice received biotin-conjugated polywraplex. The result of Figure 8c suggests that the positive charges of bare polyplexes were responsible for liver capture and the surface-conjugated biotin facilitated cancer cell targeting. This circulation-time dependence confirmed our earlier claim that the self-assembled triblock copolymer membrane is stable enough to ensure in vivo circulation and

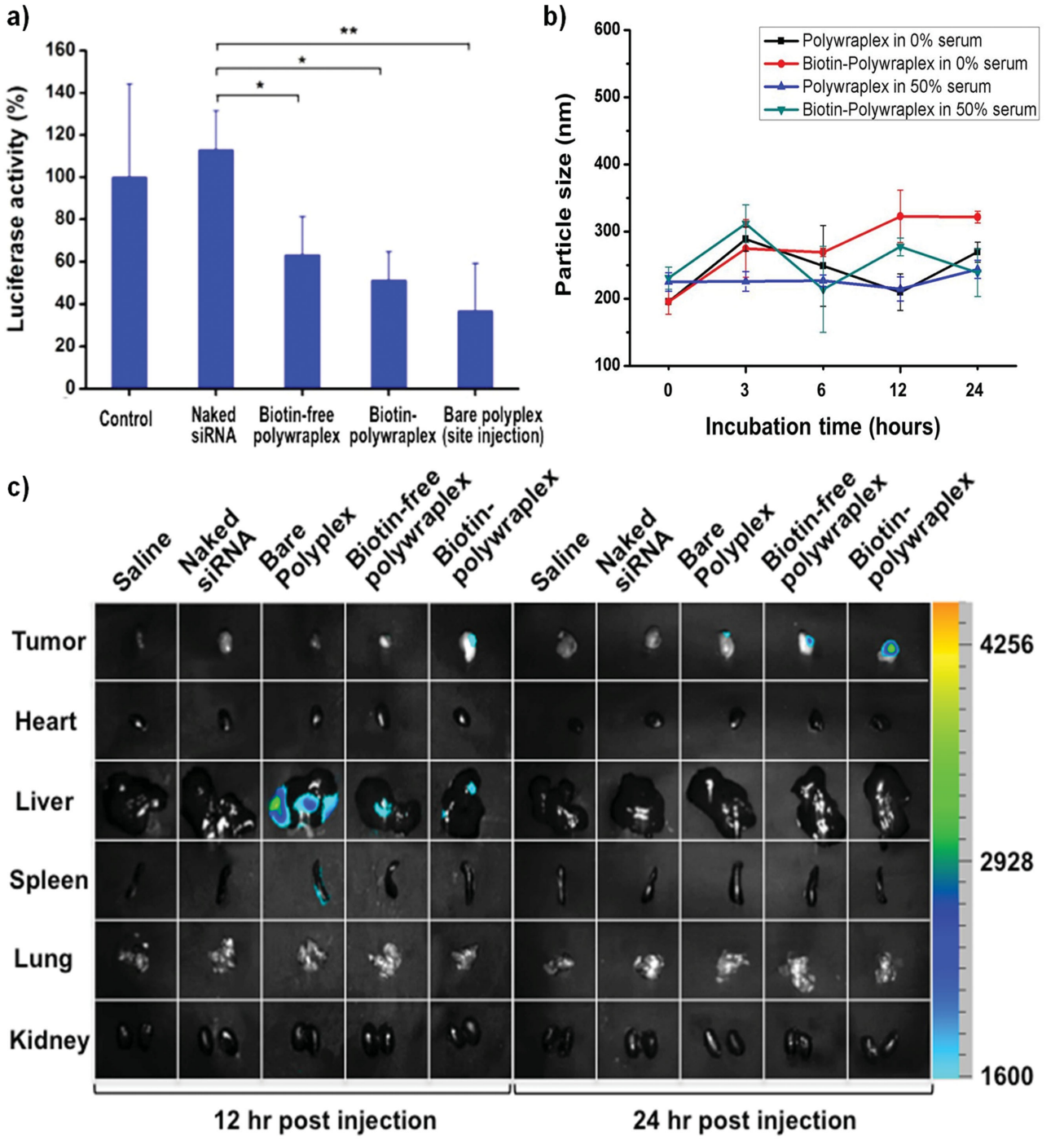

Figure 8. a) In vivo efficacy of various siRNA dosage regimes in silencing luciferase gene stably expressed in SMMC-7721 cells implanted in BALB/c nude mice. The dosage regimes were IV injections of saline (the negative control), naked siRNA, biotin-free polywraplex with siRNA and biotin–polywraplex loaded with siRNA; and intratumor injection of siRNA loaded polyplex (the positive control, N/P ratio 50). Polyplex and polywraplex core were formed of siRNA and polyspermine imidazole-4,5 imine(PSI). *$p < 0.05$ and **$p < 0.01$ versus naked siRNA mice; $n = 6$ per group; data are means±SD. b) Particle sizes of polywraplexes and biotin–polywraplexes incubated in 0% and 50% serum up to 24 h. c) Fluorescent images of organs and tissues dissected from SMMC-7721 tumor-bearing BALB/c nude mice after intravenous injection of 0.9% NaCl, naked Cy3-siRNA, polyplexes, polywraplexes, and polywraplex with 10% biotin-PEG45-PCL20-maltotriose-COO^- in the surface membrane, respectively. Dissection was carried out 12 and 24 h after IV injection of the test formulations.

tumor cell recognition of polyplexes. In terms of more quantitative information comprising the fractions of biotin–polywraplexes and biotin-free polywraplexes retained in the tumor and liver for example, a systemic pharmacokinetic–pharmacodynamics study based a standard curve of Cy3-siRNA will be a great help.

3. Discussion

3.1. Thermodynamic Basis for Post-Polyplexing Assembly of a Unilamella Membrane

Cationic polymers may offer noncomparable convenience in packing nucleic acids into nanoparticulate forms (polyplexes) via electrostatic assembly and flexibility to chemical modification to meet respective delivery needs. As the other side of the matter, however, polyplexes formed from cationic polymers suffer from a series of thorny challenges, comprising nonspecific adsorption to cells due to their excess charges, and dynamic structure that leads to aggregation at neutral potential and leaking of siRNA. Covalent conjugation and nanoencapsulation in tempts to functionalize and stabilize polyplexes for intercellular targeting encountered some difficulties that compromise gene packing efficiency, flexibility for targeting agent selection, or formulation easiness.[8–14,24–27] These unsatisfied efforts lead us to consider a "self-consist" design of a synthetic nucleic acid carrier to achieve biofunctionality and structural simplicity simultaneously.

The present method of utilizing rationally designed triblock copolymers to functionalize polyplexes met all the above criteria at once in a series of in vitro and in vivo assays. Normally, triblock copolymers with two hydrophilic and one hydrophobic blocks such as the one in the present study, $mPEG_{45}$-PCL_{20}-maltotriose-COO^-, tend to aggregate micelles in water. In the presence of cationic polyplexes however, $mPEG_{45}$-PCL_{20}-maltotriose-COO^- aligned at the surface of each oppositely charged polyplex to form a stable unilamella membrane instead of micelles. The charge–charge interaction between the anionic copolymer and cationic polyplex surface and the alignment of the hydrophobic center block within the copolymer membrane became self-consisting to each other under the 2D geometry. This thermodynamically favored conformation ensured the stability of the unilamella membrane of $mPEG_{45}$-PCL_{20}-maltotriose-COO^- around each polyplex.

3.2. Practical Significance of Stable Unilamella Copolymer Membrane Around Polyplex

More importantly, this conformational preference brought a number of practical aids required for pharmaceutically feasible gene carriers. First, the thermodynamically stable triblock copolymer membrane may effectively condense, isolate, and protect the siRNA core against prephagocytic leaking and dissociation. The thermodynamic-driven self-assembly does not only enable nonreactive and solvent-free formulation, but also offer a broad applicability to wrap a cationic polyplex of any content efficiently. Finally, cell-targeting agents for variety of cell types may be conjugated to the membrane-forming copolymer and immobilized on the carrier surface with optimized surface population simply by blending in the target-agent-free copolymers.

The particle sizes of the polywraplexes presented in this report were around 200 nm, considerably larger than the optimal for efficient nucleic acid delivery. This is mainly due to the intrinsic sizes of the polyplex core, which were formed by random aggregation between the linear cationic polymer and linear nucleic acids. There are several reported method to form polyplex of reduced sizes,[15,27] and the surface-guided assembly of polywraplex membrane should be adaptable to small size polyplexes. In fact, polyplex formed from single-molecule cationic polymer with small and defined particle size is being developed in our lab as an essential part of our nucleic acid delivery. This report, however, addresses the aspect of surface assembly and intercellular trafficking.

3.3. Are the Lack of Rationally Designed Carriers the Key Hurdle for Nucleic Acid Medicines?

Numerous synthetic carriers formed from a variety of lipids, polymers, as well as inorganic nanoassemblies have been reported in the literature, among which many have been approved for clinic trials over the last decade. However, a practically feasible choice, especially that for systemic delivery of nucleic acids, has yet to be recognized with likelihood. The efforts paid for the rational design and chemical assembly seem to be far from sufficient according to our observation. Many biologic assays and even clinic trials utilized synthetic carriers designed with insufficient biological and chemical rationales, such as missing some essential functions or lacking metabolizing pathways, for instance.[42] Since some viruses may efficiently transfect nucleic acids into target cells, the chemical mechanisms to construct effective synthetic carriers should be available in the universe. To our opinion, a carrier system of sufficiently rational design should achieve the goal of turning nucleic acids from therapeutic actives to medicines.

4. Conclusion

The thermodynamically stable and easy-to-formulate polywraplex demonstrated in this report may not provide the solutions to all the standing challenges as its current form. But the system offers a great flexibility and convenience for being equipped with variety of functional components for both inter- and intracellular delivery of nucleic acids.

5. Experimental Section

Synthesis of the mPEG-PCL-Maltotriose-COO⁻: The reactants, $mPEG_{45}$-OH (2g, 0.001 mol) and ε-carprolactone (ε-CL, 2.283 g, 0.02 mol) were added in anhydrous toluene containing stannous 2-ethylhexanoate ($Sn(Oct)_2$) as the catalysts, and allowed to react under a high-purity nitrogen atmosphere at 120 °C for 24 h to form $mPEG_{45}$-PCL_{20}. The desired polymer was precipitated by diethyl ether and washed for three times, followed by drying in vacuum at room temperature for 24 h. The harvested $mPEG_{45}$-PCL_{20} (0.2 g, 0.05 mmol dissolved in anhydrous CH_2Cl_2, 10 mL) was then dropped into oxalyl chloride (0.065 g, 0.5 mmol dissolved in small amount of anhydrous CH_2Cl_2) touched with a liquid nitrogen bath. After stirring for 2 h, the reactants were warmed up to room temperature and proceeded for additional 12 h. The resulting solution was evaporated to remove the solvent and excess oxalyl chloride to harvest the activated $mPEG_{45}$-PCL_{20} (PEG_{45}-PCL_{20}-COCl). The product (dissolved in 5 mL anhydrous CH_2Cl_2) was then added dropwise to excess maltotriose (0.08 g, 0.16 mmol, dissolved in 1 mL anhydrous *N*,*N*-Dimethylformamide (DMF) together with small amount of pyridine) in an ice bath, followed by stirring at

room temperature for 12 h. The reactant solution was evaporated again to remove solvents and redissolved in water, followed by dialysis through a membrane with cutoff molecular weight of 3500 for 24 h. The dialysate ($mPEG_{45}$-PCL_{20}-maltotriose) was lyophilized (Christ Alpha 1–2 LD Freeze dryer, Germany) for the next step. As the final step, the harvested triblock copolymer, $mPEG_{45}$-PCL_{20}-maltotriose (0.09 g, 0.02 mmol, dissolved in 10 mL anhydrous CH_2Cl_2), was dropped slowly to excess oxalyl chloride (maintain the molar ratio of 10 per hydroxyl groups during the reaction) in an ice bath to ensure complete conjugation of each hydroxyl by single oxalyl chloride. After removing unreacted oxalyl chloride by evaporation, the residue was treated in water in an ice bath for 6 h to hydrolyze the dangling acyl chloride of the conjugated oxalyl chlorides to carboxyl groups. The excess reactants were washed with 5 mL water and the remaining was lyophilized to a white powder prior to storage at –20 °C under dry condition.

Synthesis of the Biotin-PEG-PCL-Maltotriose-COO⁻: As the first step, biotin (0.244 g, 1.0 mmol, dissolved in 3 mL dimethylsulfoxide (DMSO)) was activated by mixing with *N*-hydroxysuccinimide (NHS, 0.138 g, 1.20 mmol) and BOP (0.531 g, 1.20 mmol), both dissolved in DMF, and reacting in the presence of equivalent amount of triethylamine (Et_3N) at room temperature in a high-purity nitrogen atmosphere. The reaction was terminated after 36 h based on TLC monitoring, followed by removing DMF under reduced pressure. The activated biotin, biotin-NHS was purified by precipitating with isopropanol, redissolving in DMSO, and recrystallizing in isopropanol and methanol consequently. Then, biotin-NHS (0.34 g, 1 mmol) was added into NH_2-PEG-COOH (1 g, 0.5 mmol, dissolved in 2 mL acetonitrile and 1 mL CH_2CL_2) in the presence of 80 µL Et_3N, and stirred under nitrogen atmosphere at room temperature over night. The product, biotin-PEG-COOH (or biotin-CO-NH-PEG-COOH), was purified by precipitating with diethyl ether, recrystallizing in hot 2-propanol (70 °C), and drying in vacuum at room temperature and dried for 24 h. Biotin-PEG_{45}-PCL_{20}-COOH was synthesized by ring-opening polymerization of ε-caprolactone using biotin-PEG-COO^- as the initiator instead of mPEG-COO^- under the same condition. Then, biotin-PEG_{45}-PCL_{20}-COOH (0.05 g, 0.012 mmol) was dropped into excess amount of maltotriose (0.050 g, 0.099 mmol) in the presence of BOP (0.038 g, 0.086 mmol) as the coupling agent and Et_3N as a catalyst. The reaction was allowed to proceed in an anhydrous atmosphere at room temperature for 24 h. The products were purified by dialysis using a cellulose membrane with a cutoff size of 3500 to remove excess maltotriose and small fragments prior to lyophilization. Biotin-PEG_{45}-PCL_{20}-maltotriose (0.04 g, 0.009 mmol) was finally added into excess amount of oxalic acid (0.1 g, 1.111 mmol dissolved in DMF) in the presence of BOP(0.05 g,0.113 mmol)and Et_3N to carboxylate the hydroxyls of the sugar block. The reaction was proceeded in an anhydrous atmosphere at room temperature for 24 h and then evaporated to remove the solvent. The obtained viscous product was redissolved in chloroform (1 mL) and precipitated by adding methanol to remove the excess oxalic acid.

Formation and Characterization of Polywraplex: The polyplex core to form polywraplexes was prepared by adding cationic polymers (PEI-25KD for in vitro test and PSI for in vivo experiment) into a solution of fluorescently (carboxyfluorescein) labeled siRNA at a predetermined W/W ratio. The triblock copolymer, $mPEG_{45}$-PCL_{20}-maltotriose-COO^-, was added to the polyplex solution at the predetermined mass ratios, followed by mixing (for 30 s) and incubating (12 h).The particle size and zeta potential of the formed polywraplexes were measured using dynamic laser scattering (Brookhaven, USA). Form fluorescent imaging, the polywraplexes were suspended in a PVA solution (5%–15% in concentration), loaded on a glass slide, and gelled via a freeze–thaw treatment. The polywraplex particles immobilized in the PVA gel were to a fluorescent microscope (Olympus BX61) and photographed consequently using incident lasers, 460–495 nm and 530–550 nm in wave length. Morphology of the polywraplexes was imaged using a transmission electron microscopic (TEM, JEM 2010 system JEOL, Japan).

Cytotoxicity by MTT Assay: The cytotoxicity of the block polymer and formed polywraplexes was examined by adding the samples into HepG2, HeLa, SMMC-7721,HL7702, and BRL-3A cells, followed by standard MTT assay. In brief, the cells were seeded in a 96-well plate at a density of 8000 per well in 100 µL of Dulbecco's modified Eagle's medium (DMEM) containing 10% FBS overnight. The polymer or polywraplexes were dissolved/dispersed in fresh, serum-free, and phenol red-free DMEM and added into the cells, followed by incubation for 4 h. The medium was replaced with fresh DMEM, and 25 µL of 3-(4,5-Dimethyl-2-thiazolyl)-2,5-diphenyl-2H-tetrazolium bromide(MTT) solution (5 mg mL^{-1}) was added into the cells. After further incubation for 6 h, 100 µL DMSO was added into each well until the formazan crystal was dissolved completely. Normalized cell viability was determined by the absorbance of the samples at 570 nm using a SpectraMax M3 Multi-Mode Microplate Reader.

Protective Effect of TriBlock Copolymer Membrane of Polywraplex: PEG_{45}-PCL_{20}-maltotriose-COO^- and PEG-DEX-COO^- were added, respectively, to polyplexes, followed by incubation with calf thymus DNA (0.05 times to siRNA in mass ratio) or fetal bovine serum (FBS) solution for 48 h. Samples were taken at each programmed time and subjected to electrophoresis with nucleic acid markers of known molecular weight.

In Vitro Gene Silencing Assay: Polywraplexes loaded with anti-pGL3 luciferase siRNA in the core and biotin at the surface were prepared by self-assembling as above. The fractions of biotin-conjugated triblock copolymer were 0%, 10%, 20%, 30%, 40%, and 50%, respectively. For in vitro assays, SMMC-7721 cells that stably express GL3 luciferase gene were seeded in a 24-well plate at a density of 6×10^4 cells per well in 500 µL DMEM media containing 10% FBS at 37 °C in a 5% CO_2 incubator overnight. Polywraplexes of various biotin populations were added to the cell culture, respectively, with naked siRNA as the reference, and incubated at 37 °C in serum-free medium for 4 h and in 10% FBS medium for additional 48 h. The transfected cells were then washed with PBS solution and lysed with 1× cell culture lysis buffer (Promega), followed by centrifugation at 12 000 rpm for 3 min (Eppendorf 5810 R Centrifuge, Germany). The supernatant was mixed with substrate (Luciferase Assay System, Promega) at a 1:1 ratio and the luminescence was measured by a single-tube luminometer (Sirius-Single Tube Luminometer from Berthold Detection Systems GmbH). The protein concentrations were determined using a Micro BCA Protein Assay Kit (Thermo Scientific Pierce). Luciferase activity of a sample was normalized on protein concentration and then expressed as the percent decrease of luminescence intensity compared to the untreated group as control.

In Vivo Gene Silencing Assay: Nude BALB/c mice were implanted with SMMC-7721 cancer cells in the back to create the model animal bearing a tumor, ≈200 mm^3 in size. The dosage forms of naked anti-pGL3 siRNA, biotin-free polywraplex and biotin–polywraplex (10% biotin-PEG_{45}-PCL_{20}-maltotriose-COO^-) were injected to the model mice at the dose of 0.5 mg kg^{-1} (in 200 µL saline) through the tail vein. Bare polyplex was given by site injection to the tumor tissue as the positive control. To avoid the effect of polymer toxicity, PSI was used instead of PEI to form the polyplex core of polywraplexes. The mice were sacrificed after 48 h and the tumor tissue was dissected, homogenized in liquid nitrogen, and lysated. Luciferase expression was measured and the silencing efficiency was calculated relative to saline group as 100%.

Tissue Distribution of Polywraplexes: Five dosage regimes, saline, naked Cy3-labeled siRNA, bare-polyplex, biotin-free polywraplex, and biotin–polywraplex (10% biotin-PEG_{45}-PCL_{20}-maltotriose-COO^-) were injected intravenously at the dose of 0.5 mg Kg^{-1} (in 200 µL saline) via the tail vein. After systemic injection, the mice were sacrificed 12 and 24 h after the dosage form administration, respectively. The main organs and tumor tissue were dissected and imaged under a fluorescent microscope (ZhongKeKaiSheng Medical Technology Co., Ltd, China).

Supporting Experiments: The procedures and results of the experiments not shown in the main text were summarized in Supporting Information associated with this manuscript. The supporting information obtained from the supporting experiments include mass spectrum of the biotin-NHS, size distribution and TEM image of polywraplexes, protective effect of the PCL hydrophobic layer to siRNA, transfection activities of polywraplexes in cellular assays, and silencing

efficiency characterization of PSI-siRNA-core polywraplex in SMMC-7721 (stably expressing GL3 luciferase gene) tumor-bearing mice.

Animal Welfare: Usage of experimental mice in this study was approved by the animal welfare committee, SJTU School of Pharmacy.

Supporting Information

Supporting Information is available from the Wiley Online Library or from the author.

Acknowledgements

T.J. invented the initial idea, designed the experiments together with X.G., and revised the manuscript. X.G. carried out the experiments and drafted the manuscript. S.D. helped animal trials, F.W. involved in discussion during this study. J.F. helped determining the size of PEG-DEX-COO$^-$ wrapped polyplexes. H.Z. helped to prepare fluorescent images. This study was financially supported by the grants of Natural Science Foundation of China (Nos. 81373366 and 81373352). The authors also appreciate the generous help from faculties of Instrumental Analysis Centre (IAC) of Shanghai Jiao Tong University.

Received: February 23, 2015
Revised: May 10, 2015
Published online: June 9, 2015

[1] B. L. Davidson, P. B. McCray Jr., *Nat. Rev. Genet.* **2011**, *12*, 329.
[2] K. Gavrilov, W. M. Saltzman, *Yale J. Biol. Med.* **2012**, *85*, 187.
[3] H. Yin, R. L. Kanasty, A. A. Eltoukhy, A. J. Vegas, J. R. Dorkin, D. G. Anderson, *Nat. Rev. Genet.* **2014**, *15*, 541.
[4] O. M. Merkel, T. Kissel, *J. Controlled Release* **2014**, *190c*, 415.
[5] D. Shu, Y. Shu, F. Haque, S. Abdelmawla, P. Guo, *Nat. Nanotechnol.* **2011**, *6*, 658.
[6] F. Haque, D. Shu, Y. Shu, L. S. Shlyakhtenko, P. G. Rychahou, B. M. Evers, P. Guo, *Nano Today* **2012**, *7*, 245.
[7] E. F. Khisamutdinov, D. L. Jasinski, P. Guo, *ACS Nano* **2014**, *8*, 4771.
[8] H. J. Kim, K. Miyata, T. Nomoto, M. Zheng, A. Kim, X. Liu, H. Cabral, R. J. Christie, N. Nishiyama, K. Kataoka, *Biomaterials* **2014**, *35*, 4548.
[9] N. Cao, D. Cheng, S. Zou, H. Ai, J. Gao, X. Shuai, *Biomaterials* **2011**, *32*, 2222.
[10] C. Q. Mao, J. Z. Du, T. M. Sun, Y. D. Yao, P. Z. Zhang, E. W. Song, J. Wang, *Biomaterials* **2011**, *32*, 3124.
[11] E. Mastrobattista, R. H. Kapel, M. H. Eggenhuisen, P. J. Roholl, D. J. Crommelin, W. E. Hennink, G. Storm, *Cancer Gene Ther.* **2001**, *8*, 405.
[12] C. Dohmen, D. Edinger, T. Fröhlich, L. Schreiner, U. Lächelt, C. Troiber, J. Rädler, P. Hadwiger, H.-P. Vornlocher, E. Wagner, *ACS Nano* **2012**, *6*, 5198.
[13] R. B. Shmueli, D. G. Anderson, J. J. Green, *Expert Opin. Drug Delivery* **2010**, *7*, 535.
[14] Y.-C. Tseng, S. Mozumdar, L. Huang, *Adv. Drug Delivery Rev.* **2009**, *61*, 721.
[15] M. E. Davis, *Mol. Pharm.* **2009**, *6*, 659.
[16] X. Z. Yang, J. Z. Du, S. Dou, C. Q. Mao, H. Y. Long, J. Wang, *ACS Nano* **2012**, *6*, 771.
[17] T. Smyth, K. Petrova, N. M. Payton, I. Persaud, J. S. Redzic, M. W. Graner, P. Smith Jones, T. J. Anchordoquy, *Bioconjugate Chem.* **2014**, *25*, 1777.
[18] R. J. Lee, L. Huang, *J. Biol. Chem.* **1996**, *271*, 8481.
[19] M. E. Davis, J. E. Zuckerman, C. H. Choi, D. Seligson, A. Tolcher, C. A. Alabi, Y. Yen, J. D. Heidel, A. Ribas, *Nature* **2010**, *464*, 1067.
[20] A. S. Balte, P. K. Goyal, S. P. Gejji, *J. Chem. Pharm. Res.* **2012**, *4*, 2391.
[21] W. F. Lai, *Biomaterials* **2014**, *35*, 401.
[22] E. Kim, J. Yang, H.-O. Kim, Y. An, E.-K. Lim, G. Lee, T. Kwon, J.-H. Cheong, J.-S. Suh, Y.-M. Huh, *Biomaterials* **2013**, *34*, 4327.
[23] Z. J. Deng, S. W. Morton, E. Ben-Akiva, E. C. Dreaden, K. E. Shopsowitz, P. T. Hammond, *ACS Nano* **2013**, *7*, 9571.
[24] J. Li, Y. C. Chen, Y. C. Tseng, S. Mozumdar, L. Huang, *J. Controlled Release* **2010**, *142*, 416.
[25] J. Li, Y. Yang, L. Huang, *J. Controlled Release* **2012**, *158*, 108.
[26] S. K. Cho, Y. J. Kwon, *J. Controlled Release* **2011**, *150*, 287.
[27] J. Li, X. Yu, Y. Wang, Y. Yuan, H. Xiao, D. Cheng, X. Shuai, *Adv. Mater.* **2014**, *26*, 8217.
[28] S. Duan, W. Yuan, F. Wu, T. Jin, *Angew. Chem. Int. Ed.* **2012**, *51*, 7938.
[29] J. Shi, Z. Xiao, A. R. Votruba, C. Vilos, O. C. Farokhzad, *Angew. Chem. Int. Ed.* **2011**, *50*, 7027.
[30] B. Romberg, W. E. Hennink, G. Storm, *Pharm. Res.* **2008**, *25*, 55.
[31] Y. Sheng, C. Liu, Y. Yuan, X. Tao, F. Yang, X. Shan, H. Zhou, F. Xu, *Biomaterials* **2009**, *30*, 2340.
[32] J. Van Steenis, E. van Maarseveen, F. Verbaan, R. Verrijk, D. Crommelin, G. Storm, W. Hennink, *J. Controlled Release* **2003**, *87*, 167.
[33] G. W. Jin, H. Koo, K. Nam, H. Kim, S. Lee, J. S. Park, Y. Lee, *Polymer* **2011**, *52*, 339.
[34] D. N. Heo, D. H. Yang, H. J. Moon, J. B. Lee, M. S. Bae, S. C. Lee, W. J. Lee, I. C. Sun, I. K. Kwon, *Biomaterials* **2012**, *33*, 856.
[35] F. Gu, L. Zhang, B. A. Teply, N. Mann, A. Wang, A. F. Radovic-Moreno, R. Langer, O. C. Farokhzad, *Proc. Natl. Acad. Sci. U.S.A.* **2008**, *105*, 2586.
[36] H. Shmeeda, D. Tzemach, L. Mak, A. Gabizon, *J. Controlled Release* **2009**, *136*, 155.
[37] X. Liang, X. Li, J. Chang, Y. Duan, Z. Li, *Langmuir* **2013**, *29*, 8683.
[38] H. Nakamura, F. Jun, H. Maeda, *Expert Opin. Drug Delivery* **2015**, *12*, 53.
[39] U. Prabhakar, H. Maeda, R. K. Jain, E. M. Sevick Muraca, W. Zamboni, O. C. Farokhzad, S. T. Barry, A. Gabizon, P. Grodzinski, D. C. Blakey, *Cancer Res.* **2013**, *73*, 2412.
[40] V. Torchilin, *Adv. Drug Delivery Rev.* **2011**, *63*, 131.
[41] A. D. Wong, M. Ye, M. B. Ulmschneider, P. C. Searson, *PLoS One* **2015**, *10*, e0123461.
[42] S. D. Li, L. Huang, *Biochim. Biophys. Acta* **2009**, *1788*, 2259.